(also Table 5-1) to correct each segment of observed groundwater drawdown using the equation:

$$s'(t) = s(t) - s(0) - E\left[H(0)_0 - H(t)\right] + s'(0) \qquad (5\text{-}15)$$

where

$s'(\tau)$	=	Corrected groundwater drawdown for the segment [L]
$s'(0)$	=	Corrected groundwater drawdown at the start of the segment [L]
$s(\tau)$	=	Observed groundwater drawdown for the segment [L]
$s(0)$	=	Observed groundwater drawdown at the start of the segment [L]
$H(\tau)$	=	Tidal elevation for the segment [L]
$H(0)$	=	Tidal elevation at the start of the segment [L]
E	=	Tidal efficiency for the segment [dimensionless]
τ	=	Time since beginning of the segment [T]

(6) The tidal correction procedure is repeated for all segments of the tidal and groundwater drawdown record.

5.1.4.2 Approach Based on the Best-Fit Equation of Groundwater Tidal Fluctuation

In the second approach for tidal correction of groundwater drawdown data, a tidal influence curve (best-fit equation) is generated for the period of the pumping test that reflects only tidal fluctuations. These tidal influence curves are generated for data from each of the observation wells. Using this approach, fluctuations in groundwater levels calculated from the tidal influence curve are subtracted from the observed drawdown data collected during the pumping test. The corrected drawdown can then be used to calculate aquifer parameters.

The tidal influence curves for observation wells within the radius of influence during a pumping test can be derived from the tidal influence curves for data from wells outside the radius of influence or from tidal curves for the bay tide. Tidal data collected at the observation wells before or after the pumping test cannot be used because the bay tide changes significantly with time. During the pumping test, tidal fluctuation at different wells within the pumping aquifer is generally a function of aquifer hydraulic properties and distance from the shoreline but not a function of time, as described in Equations 5-2 and 5-3.

In general, the tidal influence curve at a monitoring well is described as a series of sinusoidal (or cosine) functions as follows:

$$f(t) = A + \sum_{i=1}^{n} B_i \sin[\frac{2p}{T_i}(t + t_i)] \qquad (5\text{-}16)$$

where

A = A constant related to the difference between groundwater and bay tide elevations [L]

B_i = The amplitude of the i^{th} tidal constituent [L]

T_i = The period of the i^{th} tidal constituent [T]

τ_i = The phase of the i^{th} tidal constituent[T]

The amplitude, period, and phase of the tidal function in groundwater are related to the tidal efficiency and time lag of the aquifer and the same parameters of the bay tidal constituents. The bay tidal constituents in turn are caused by the rotation of the Earth about the sun, the moon about the Earth, and the Earth on its axis. The amplitude, period, and phase of each tidal constituents (waves) of the tidal influence function can be calculated through harmonic analysis, which is commonly used to predict ocean tides at various locations in the United States. The phase of the ocean tide is determined by the starting point of the prediction, and the phase of groundwater tidal influence is a function of the starting point of the calculation and time lag behind the ocean tide.

Groundwater level at well MW-20 was observed using a pressure transducer during the entire period of the aquifer test (including step drawdown and constant discharge pumping tests). Well MW-20 is located approximately 800 feet from the NoVOCs™ pumping well and about 140 feet from San Diego Bay. This well is clearly outside the radius of pumping influence. Therefore, the second approach (best-fit equation) was developed using groundwater level data for well MW-20.

The tidal correction procedures for the pumping test drawdown data based on the best-fit equation approach is described as follows:

(1) Plot the groundwater level data collected from well MW-20. Based on Equation 5-16, a best-fit tidal curve (as a sinusoidal equation) can be obtained through harmonic analysis. The plot and best-fit tidal curve are presented in Figure 5-2. The correlation coefficient

(R^2) of the best-fit equation (tidal curve) is 0.96. The tidal curve for MW-20 is described as:

$$f_{MW-20}(t) = 3.60 + 0.21\sin(\frac{2p}{25.76}t) + 0.51\sin[\frac{2p}{23.78}(t-1.72)] + 0.69\sin[\frac{2p}{12.36}(t-6.87)] + 0.29\sin[\frac{2p}{11.89}(t-8.92)] \quad (5\text{-}17)$$

(2) Select a time period when the pumping impact is insignificant (from August 1 through 4, 1998, after the deep aquifer zone step drawdown tests), and compare data for well MW-20 with the bay tide and groundwater level data collected from other observation wells (Figures 5-3 through 5-10)

(3) Based on Equation 5-17 and Figure 5-3, generate the tidal influence curve for well MW-45: the elevation constant (A) is calculated

(4) Based on the difference between the average groundwater elevations in wells MW-20 and MW-45; the amplitude constants (B_i) are calculated based on the difference in tidal efficiency between the two wells; the tidal period constants (T_i) are kept the same; and phase constants (τ_i) are adjusted based on the starting time and the different time lags between the two wells. The tidal influence curve for well MW-45 during the period of the constant discharge pumping test is described as follows:

$$f_{MW-45}(t) = 5.00 + 0.057\sin[\frac{2p}{25.76}(t+0.79)] + 0.12\sin[\frac{2p}{23.78}(t-0.05)] + 0.29\sin[\frac{2p}{12.36}(t-7.94)] + 0.15\sin[\frac{2p}{11.89}(t-8.11)] \quad (5\text{-}18)$$

(5) Repeat Steps 3 and 4 to obtain the tidal influence curves for data from wells MW-46, MW-47, MW-48, MW-49, MW-52, MW-53, and MW-54. Equation 5-17 and Figures 5-3 through 5-10 are used for determining the tidal influence functions. The tidal influence curves for these wells during the constant discharge pumping test are described by the following equations:

$$f_{MW-46}(t) = 4.77 + 0.05\sin[\frac{2p}{25.76}(t+0.31)] + 0.14\sin[\frac{2p}{23.78}(t-1.42)] + 0.26\sin[\frac{2p}{12.36}(t-8.13)] + 0.16\sin[\frac{2p}{11.89}(t-8.32)] \quad (5\text{-}19)$$

$$f_{MW-47}(t) = 4.51 + 0.06\sin[\frac{2p}{25.76}(t + 2.95] + 0.142\sin[\frac{2p}{23.78}(t + 0.63)] + 0.283\sin[\frac{2p}{12.36}(t - 7.78)] + 0.163\sin[\frac{2p}{11.89}(t - 7.66)] \quad (5\text{-}20)$$

$$f_{MW-48}(t) = 4.71 + 0.12\sin[\frac{2p}{25.76}(t + 1.63)] + 0.163\sin[\frac{2p}{23.78}(t + 0.55)] + 0.26\sin[\frac{2p}{12.36}(t - 8.60)] + 0.19\sin[\frac{2p}{11.89}(t - 9.15)] \quad (5\text{-}21)$$

$$f_{MW-49}(t) = 4.51 + 0.02\sin[\frac{2p}{25.76}(t + 0.30)] + 0.06\sin[\frac{2p}{23.78}(t - 0.78)] + 0.266\sin[\frac{2p}{12.36}(t - 8.09)] + 0.167\sin[\frac{2p}{11.89}(t - 8.38)] \quad (5\text{-}22)$$

$$f_{MW-52}(t) = 4.76 + 0.02\sin[\frac{2p}{25.76}(t + 1.86)] + 0.08\sin[\frac{2p}{23.78}(t - 0.31)] + 0.205\sin[\frac{2p}{12.36}(t - 7.91)] + 0.08\sin[\frac{2p}{11.89}(t - 9.14)] \quad (5\text{-}23)$$

$$f_{MW-53}(t) = 4.49 + 0.02\sin[\frac{2p}{25.76}(t + 1.86)] + 0.14\sin[\frac{2p}{23.78}(t - 1.42)] + 0.26\sin[\frac{2p}{12.36}(t - 8.13)] + 0.16\sin[\frac{2p}{11.89}(t - 8.32)] \quad (5\text{-}24)$$

$$f_{MW-54}(t) = 5.04 + 0.035\sin[\frac{2p}{25.76}(t + 0.31)] + 0.103\sin[\frac{2p}{23.78}(t - 1.08)] + 0.275\sin[\frac{2p}{12.36}(t - 8.13)] + 0.16\sin[\frac{2p}{11.89}(t - 8.32)] \quad (5\text{-}25)$$

(6) Calculate tidal fluctuation in groundwater using the above tidal influence equations for data from all observation wells. Subtract the tidal fluctuation from the observed groundwater elevations, and calculate tidally corrected drawdown from the tidally corrected groundwater elevations. Using data for well MW-45 as example, the corrected drawdown is calculated using the following equation:

$$s^*(t) = [h(0) - f_{MW-45}(0)] - [h(t) - f_{MW-45}(t)] \quad (5\text{-}26)$$

where

s*(t) = Tidally corrected groundwater drawdown [L]

h (0) = Observed groundwater elevation at the beginning of the pumping test [L]

h (t) = Observed groundwater elevation during the pumping test [L]

f_{MW-45} (0) = Calculated groundwater elevation from the tidal influence curve at the beginning of the pumping test [L]

f_{MW-45} (0) = Calculated groundwater elevation from the tidal influence curve at the beginning of the pumping test [L]

5.1.5 Tidal Influence Correction for the Constant Pumping Test

As shown in Figures D2 through D6 in Appendix D, groundwater level data collected during the constant discharge pumping test in the upper aquifer zone showed significant tidal influence. In order to use the pumping test data to calculate aquifer hydraulic parameters, the observed groundwater drawdown must be corrected for tidal influence. The goal of the tidal influence correction is to separate groundwater drawdown caused by pumping from groundwater fluctuations caused by tidal influence, only the pumping-induced groundwater drawdown is used to calculate aquifer parameters.

Two tidal influence correction approaches are developed and discussed in Section 5.1.4. Both approaches are used to correct the drawdown data collected during the constant discharge pumping test in the upper aquifer zone. The two key tidal influence parameters, tidal efficiency and time lag, are applied in the first approach to derive fluctuations in groundwater caused by tides at the observation wells. The parameter values are initially calculated from the April 1998 tidal study data. Because the bay tide during the pumping test (July/August 1998) was different from the tide in April 1998, the parameters are adjusted to provide the best results of tidal influence correction. Table 5-2 shows the adjusted tidal efficiency and time lags used for the tidal influence correction.

Observed San Diego Bay tide and groundwater levels in well MW-20, the simulated tidal influence (curves), and observed groundwater levels for well MW-45 during the constant discharge pumping test are compared in Figure 5-11. The figure shows that the tidal influence decreased with distance from the bay, and that the simulated tidal influences using the two different approaches are similar.

Figures 5-12 through 5-19 compare the observed and corrected groundwater drawdown data at different observation wells for the constant discharge pumping test. As shown in these figures, the original observed groundwater drawdown graphs indicate significant tidal influence. After correction for tidal influence, the groundwater drawdown curves show typical groundwater level drawdown caused by pumping. The figures also show that the tidal influence corrections using the two different approaches are generally in close agreement. The corrected groundwater drawdown data using the linear relationship approach are applied in Section 5.3 to calculate aquifer parameters.

In summary, two new approaches for tidal correction of groundwater drawdown data collected during a pumping test have been developed. The corrected drawdown data using both approaches correlated reasonably well with each other and reflect typical pumping test responses. Some uncertainties associated with both tidal correction approaches include impact of aquifer heterogeneity, differences in tidal fluctuation during different tidal periods (tidal cycles), and interpolation of tidal data to match frequent data records at the early stage of the pumping test.

5.2 CALCULATION OF SPECIFIC CAPACITY AND WELL EFFICIENCY

This section presents the calculations of specific capacity and well efficiency for the NoVOCs^{TM}well. The calculations are based on water level data collected from the step-drawdown test conducted in the upper screened portion of the well (screened in the upper aquifer zone), the step-drawdown conducted in the lower screened portion (screened in the deep aquifer zone), and the water injection test conducted in the upper screened portion.

5.2.1 Specific Capacity Calculation

Specific capacity of a pumping well is calculated based on (1) the pumping rate and measured maximum drawdown for pumping tests, or (2) the injection rate and maximum water level rise for injection tests (assuming the drawdown and water level rise had stabilized) during each test step. The upper aquifer zone step-drawdown test was conducted in three steps. The upper aquifer zone step-injection test and the deep aquifer zone step-drawdown pumping test were each conducted in four steps. The specific capacity is calculated using the following equation:

$$q_i = \frac{Q_i}{s_i} \qquad (5\text{-}27)$$

where

q_i = Specific capacity [L^2T^{-1}]

Q_i = Pumping (or injection) rate [L^3T^{-1}]

s_i = Maximum drawdown (or water level rise) [L]

Figures C1, E1, and F1 (Appendices C, E, and F) show the water levels during the step tests. Table 5-3 shows the step test data and calculated specific capacities for each step of the tests. Based on the upper aquifer step-drawdown test, specific capacity of the NoVOCs™well calculated for various steps ranges from 1.35 to 1.70 gpm/ft, with the average of 1.48 gpm/ft. The upper aquifer injection test shows similar results, and the calculated specific capacity ranges from 1.45 to 1.57 gpm/ft, with the average of 1.50 gpm/ft. The specific capacity values estimated from the deep aquifer step-drawdown test are higher than for the upper aquifer zone. The calculated specific capacity for the deep aquifer ranges from 3.02 to 3.51 gpm/ft, and the average specific capacity is 3.22 gpm.

5.2.2 Well Loss and Well Efficiency

The theory and concept of well loss and well efficiency and applied approaches for step-drawdown test data analysis have been extensively discussed in the literature. Currently, there are still different theories and approaches to calculate well efficiency. This section presents a brief evaluation of different approaches (Section 5.2.2.1) and calculation of well loss and well efficiency for the NoVOCs™well based on the step-drawdown and step-injection test data (Section 5.2.2.2).

5.2.2.1 Evaluation of Different Approaches

The discussion of well loss and well efficiency are somewhat conflicting and confusing, as reflected in the literature (Jacob 1947; Rorabaugh 1953; Driscoll 1986; and Kawecki 1995). According to Jacob (1947), total drawdown in a pumping well can be divided into two components: (1) aquifer drawdown that can be described as a linear (first order) function of pumping rate and (2) well loss (caused by turbulent flow) that can be described as an second-order function of the pumping rate, as follows:

$$s = BQ + CQ^2 \qquad (5\text{-}28)$$

where

s	=	Total drawdown (or water level rise) in the pumping (injection) well [L]
Q	=	Pumping rate [L^3T^{-1}]
B	=	Aquifer drawdown coefficient [$L^{-2}T$]
C	=	Well loss coefficient [$L^{-5}T^2$]

Rorabaugh (1953) proposed a more general empirical form of well loss that is described as a n^{th}-order function of the pumping (or injection) rate. Thus, the total drawdown can be expressed as follows:

$$s = BQ + CQ^n \tag{5-29}$$

Step-drawdown tests are commonly used to determine B, C, and n. Rorabaugh (1953) used n values ranging from 2.43 to 2.82; however, Lennox (1966) reported that n=3.5 was more suitable for his step-drawdown test data analysis. In practice, Equation 5-28 has been more widely used and the well loss component is generally considered a second-order function of the pumping rate (n=2). BQ represents aquifer drawdown caused by pumping, and CQ^2 represents the well loss. Once the coefficients B and C are determined, the well efficiency E_{well} (in percent) is calculated as follows:

$$E_{well} = \frac{s - CQ^2}{s} \times 100 \tag{5-30}$$

Driscoll (1986) pointed out that Jacob's and Rorabaugh's definitions of well loss and well efficiency were inadequate and that their assumptions that well loss is attributable to turbulent flow and aquifer drawdown is attributable to laminar flow were incorrect. Based on Driscoll (1986), a portion of the CQ^2 term might actually come from aquifer drawdown and portion of BQ term might include well losses. Driscoll's conclusion was reportedly based on testing of hundreds of wells, however, no details were given regarding the tests and data.

Kawecki (1995) concluded that traditional methods of analyzing step-drawdown test data produce information (well loss and well efficiency) that can be misleading, inaccurate, or meaningless. Kawecki's conclusion is based on the assumption that well losses include both linear and nonlinear components.

Kawecki separated the aquifer drawdown coefficient (B) into B_1 and B_2; where B_1 represents the "true aquifer drawdown" coefficient as a function of "real well radius" and time, and B_2 represents the linear well loss coefficient.

Calculating the well efficiency based on the "true aquifer drawdown" and "real well radius" is not a simple task because the "true aquifer drawdown" cannot be readily measured in most cases. Calculated aquifer drawdown is generally not accurate because of uncertainties associated with the parameters and model assumptions. The methods provided by Driscoll (1986, page 558) and Kawecki (1995) both require accurate values for aquifer and pumping well parameters. Driscoll's and Kawecki's examples show that the calculated well efficiencies based on the aquifer and pumping well parameters can have a large range of values because of uncertainties of the estimated parameter values. Therefore, the methods by Driscoll and Kawecki are inaccurate and impractical.

Dawson and Istok (1991) proposed two methods to determine the well efficiency. The first method is similar to the Driscoll (1986) method that requires calculation of the theoretical aquifer drawdown based known aquifer transmissivity and storativity values. The second method plots distance-drawdown data from at least three observation wells and extrapolates a straight fitted line to project aquifer drawdown at the pumping well. There are two problems with this method: (1) aquifer drawdown is not a linear function of distance, nor a logarithmic linear function of distance because Jacob simplification of Theis equation is not valid for short duration of step-drawdown tests; and (2) a large extrapolation will pose significant error in determining the actual aquifer drawdown at the pumping well. Both methods proposed by Dawson and Istok, therefore, are also inaccurate and impractical.

Well efficiency calculation in this study is based on the traditional concepts that well losses are caused by turbulent flow near and within the pumping well and aquifer drawdown is a result of laminar flow. The well losses can be described as a second-order function of pumping rate and aquifer drawdown is determined as a linear function of the pumping rate (Equation 5-28). For this study, it is believed that Equations 5-28 and 5-30 is adequate and applicable to calculate the well efficiency.

5.2.2.2 Calculation

Well loss and well efficiency can be calculated using graphical methods and computational approaches based on step-drawdown pumping test data. A simple graphical method that has been widely used is to plot s/Q versus Q (Bierschenk 1964). Rearranging Equation 5-28, s/Q can be expressed as:

$$\frac{s}{Q} = B + CQ \qquad (5\text{-}31)$$

Based on Equation 5-31, s/Q versus Q plots should yield a straight line with slope C and y-axis intercept B.

The disadvantages of this graphical approach are: (1) high uncertainty because multiple steps (at least three) of step-drawdown test data may not adequately fit a straight line (low correlation coefficient); and (2) calculation error will increase significantly when the pumping rate is relatively low and well loss is small (nearly a horizontal line).

The straight line graphical method is not appropriate for analyzing the NoVOCs™well step test data because s/Q versus Q plots are scattered. The data poorly match a straight line (correlation coefficient, R^2, is less than 0.62; see Figures 5-20 and 5-21). In some cases, a straight line cannot be obtained. Examples of s/Q versus Q are presented in Figures 5-20 and 5-21.

A new graphical approach developed for this investigation was therefore used instead to calculate aquifer drawdown and well loss coefficients (B and C) in this study. The observed total drawdown (s) versus pumping rate (Q) is plotted and a best-fit second order polynomial function is generated using the least-square method (Figure 5-22 through Figure 5-24). Based on Equation 5-29, parameters B and C are determined by the best-fit curves. Figures 5-22 through 5-24 show that the correlation coefficients (R^2) of the best-fit equations range between 0.97 to 0.99. For the upper aquifer injection test, water level rise is used instead of drawdown (Figure 5-23).

Well efficiency calculation results are presented in Table 5-4. As shown in the table, the calculated well efficiencies for both shallow and deep NoVOCs™wells are quite high, ranging from 77 to 99 percent. These efficiencies indicate that well losses through the well screen and sand pack are relatively low for

the pumping and injection rates used in the step tests. The well efficiency will decrease when pumping rates increase.

Table 5-4 also shows that the shallow well injection efficiency (average 97 percent) is higher than the pumping efficiency (average 82 percent). There are several explanations for the higher injection efficiency. First, the shallow well was redeveloped just before the injection test because of the inadvertent injection of turbid water from a dirty hose. The well was subsequently pumped intensively (five times the volume of water injected) to clean the well. Second, the injected water was clean tap water that was less turbid than the aquifer water being pumped. Third, uneven cuts of screen slots between the inside and the outside of the well screen may cause outward (injection) flow to be less turbulent than inward (pumping) flow.

The injection efficiency calculated using the step-injection test data is consistent with the well efficiency based on measured water level rises inside and outside of the well screen (upper piezometer data). Well efficiency was also evaluated using the dipole test data (see Section 5.5 of this report). The dipole test data may be more representative of the NoVOCs^{TM} operation efficiency because injected water was drawn directly from the deep aquifer. Conversely, the injected water used for the upper aquifer injection test was clean tap water. Clean tap water has different physical and chemical characteristics (particularly turbidity, pH, and Eh) from the aquifer water, and it may have affected the injection test results.

5.3 AQUIFER HYDRAULIC PARAMETER CALCULATION

This section analyzes the data from the constant discharge pumping test conducted in the upper screened portion of the NoVOCs^{TM} well and presents calculations of values for various aquifer hydraulic parameters. Many analytical models are available to analyze pumping test data and calculate aquifer hydraulic parameters. Different models were developed to simulate a variety of aquifer conditions. The first and most critical step in a pumping test data analysis is to select an appropriate model (or models) for the specific aquifer conditions, pumping and observation well construction, and pumping test configurations.

The analytical model for the NoVOCs^{TM} well pumping test data evaluation was selected based on the site hydrogeologic conceptual model, the pumping test configuration (including pumping and observation well construction), and the pumping test drawdown response characteristics. Section 5.3.1 summarizes the site hydrogeology and presents the site hydrogeologic conceptual model. Section 5.3.2 describes the

pumping test configuration. Section 5.3.3 discusses the drawdown response characteristics of the pumping test. Section 5.3.4 discusses selection of the analytical model, and describes the selected model and its applicability. The results of parameter calculation are discussed in Section 5.3.5.

5.3.1 Site Hydrogeologic Conceptual Model

The site hydrogeology has been discussed in Section 2.5. The site hydrogeological conceptual model for the tested aquifer is summarized as follows:

- The aquifer is a thick layer of fine sand that is generally composed of artificial fill and shallow marine-deposited sediments. The aquifer extends from the ground surface to a depth of approximately 105 feet bgs across the site.
- The aquifer is underlain by an impermeable layer (aquitard) of clay (the B clay), which forms the base of the aquifer. Several less permeable layers such as dense or silty sand and the A silt/clay exist within the aquifer in variable thicknesses (generally less than a few feet); none of these less permeable layers behave as significant aquitards because they are relatively thin and lack lateral continuity.
- Although the aquifer is heterogeneous and anisotropic in a large scale, it can be considered homogenous and horizontally isotropic within the zone of pumping influence because the grain size of the fine sand layer is relatively uniform. The aquifer is vertically anisotropic.
- The aquifer is generally under unconfined conditions. The lower portion of the aquifer below the dense sand layer may be under semiconfined conditions.
- The initial water level in the tested aquifer was observed at approximately 17 feet bgs. Groundwater generally flows to the west toward San Diego Bay; however, the groundwater gradient is small and relatively flat.
- Groundwater recharge and discharge are primarily through lateral flow. Vertical infiltration is another source of groundwater recharge. No precipitation occurred during the pumping test period; therefore, the vertical recharge is negligible.
- San Diego Bay is considered a lateral boundary of the aquifer. However, the drawdown responses from the pumping test do not reach the bay, which is approximately 1,000 feet from the test site. Consequently, boundary effects of pumping are considered insignificant.
- The aquifer is tidally influenced. Tidal influence correction may be needed for the drawdown responses in the observation wells.

5.3.2 Constant Discharge Pumping Test Configuration

Pumping test configuration is important in selecting analytical models. Construction details of the pumping and observation wells, the pumping rate and duration, and the spatial orientation of the observation wells for this pumping test study are discussed in Sections 4.1 and 4.3. The constant discharge pumping test configuration was as follows:

- Groundwater was pumped from the upper screened interval of the NoVOCs™well, which is 43 to 47 feet bgs.
- Pumping well diameter is 8 inches, and boring diameter is 14 inches (including sand pack).
- Pumping rate was kept constant at 20 gpm.
- Pumping duration was 32 hours.
- Initial groundwater level was approximately at 17 feet bgs.
- Saturated thickness of the tested aquifer was estimated at 88 feet.
- Drawdown was monitored in 10 observation wells surrounding the pumping well, but the data logger malfunctioned at two of the observation wells (MW-50 and -51).
- Distances between the observation wells and the pumping well range from 27.7 to 107.9 feet.
- Most of the observation wells have 5-foot screens, except for MW-54 which has a 40-feet screened interval.
- The observation wells are screened at various depths of the aquifer, ranging from 38 to 78 below ground surface.
- The pumping well and all of the observation wells are all partially penetrating wells.

Table 5-5 summarizes the pumping test configuration; this information was used for data interpretation and calculation of aquifer hydraulic parameters.

5.3.3 Drawdown Response Characteristics

In general, drawdown data from the pumping and observation wells are plotted in linear, semilogarithmic, and logarithmic scales. By comparing the drawdown plots with type curves, many important features of the aquifer conditions can be characterized. Some of the important features include well loss or wellbore

storage effects, pumping rate variations, leaky aquifer condition, positive (recharge) or negative (impermeable) boundaries, and delayed yield effects.

Evaluation of drawdown responses for this pumping test study is complicated because of tidal influences during the test. The magnitude of the maximum observed drawdowns in each of the observation wells is similar to the magnitude of the tidal fluctuations in the aquifer (see Figures 5-12 through 5-19). Therefore, data cannot be analyzed before tidal correction is made. The tidal influence correction procedure and corrected drawdown results were described in Section 5.1 of this report. The drawdown data analysis of all the observation wells is based on the corrected data. The pumping well drawdown (more than 16 feet) was significantly greater than the tidal fluctuations in the groundwater level (less than 0.8 feet). Consequently, the pumping well data do not need correction for tidal influence.

Table 5-6 summarizes the drawdown responses for all wells during the constant discharge pumping test. The initial response time is the time at which drawdown in an observation well is first positively identified. The water levels were affected by tidal influence, and the maximum drawdown values presented in Table 5-6 may include numerical error caused by the tidal correction.

The initial response time and maximum drawdown observation wells show that the wells constructed at different depths all responded to pumping in the upper aquifer zone. There are slight variations in response time and maximum drawdown at the well cluster nearest to the pumping well (MW-45, MW-46, and MW-47). These slight variations disappeared with distance from the pumping well, as noted in well cluster MW-48 and MW-49, with the response time increasing and maximum drawdown decreasing with depth. This type of response shows that the vertical hydraulic connection between the upper aquifer zone and lower aquifer zone is good; the dense or silty sand layers do not behave as a significant aquitard.

Table 5-6 also shows that the maximum drawdown and response time in the observation wells vary inversely with distance from the pumping well. This inverse relationship indicates that the aquifer is relatively homogeneous and isotropic in horizontal directions.

The log-log plots of the drawdown data for the observation wells (Figures 5-25 through 5-32) shows that the early data follow the Neuman type curve A closely. These early data were recorded in a short period during which the tidal influence is insignificant; therefore, tidal correction is minimal. The corrected late drawdown data clearly show the delayed yield effects that may be attributed to delayed gravity water

releases near the water table or the vertical flow component caused by partially penetrating pumping and observation wells. The late data may also include errors in the tidal influence correction.

The following summarizes the drawdown responses of the observation wells during the constant discharge pumping test:

- Drawdown responses were identified in all of the observation wells within a radius of 108 feet; positive identification of drawdown is defined as drawdown is greater than 0.01 feet (any data recorded below 0.01 feet include significant transducer and data logger error).
- Early drawdown responses in the wells show that the data plots closely follow the Theis-type curve; the intermediate and later data indicate delayed gravity yield effects.
- In horizontal directions, maximum drawdown decreases, while the response time increases, with distance from the pumping well, suggesting horizontal homogeneity and isotropy of the aquifer.
- In vertical directions, slight differences in maximum drawdown and responding time were observed among the well clusters 30 feet away from the pumping wells. The differences are less distinguishable in the well cluster 60 feet from the pumping well. These differences may indicate that vertical anisotropy exists within the tested aquifer; however, a significant or continuous aquitard probably does not exist between the upper and lower aquifer zones.

5.3.4 Selection of Analytical Model

Based on the site hydrogeologic conceptual model, the pumping test configuration, and drawdown response analysis discussed in the previous sections, the tested aquifer is considered a thick unconfined aquifer with some vertical anisotropy. Both the pumping well and observation wells partially penetrate the aquifer. Neuman's delayed yield model for partially penetrating wells in an unconfined aquifer (Neuman 1975) was selected as the most appropriate analytical model for the pumping data test analysis.

Neuman's model simulates two stages of groundwater release from an unconfined aquifer to a pumping well. At the early stage of the test, groundwater is released from the aquifer by water pressure decreases and aquifer compression. At the later stage, groundwater is primarily released by gravity drainage of the aquifer matrix (delayed yield), which usually causes a decrease in the groundwater drawdown rate.

Four parameters can be calculated by curve matching techniques used in the Neuman method: transmissivity (T), storativity (S), specific yield (S_y), and Neuman delayed yield factor (β). Aquifer transmissivity is defined as hydraulic conductivity multiplied by aquifer thickness; it measures the volume of groundwater that flows through a vertical area defined by unit width and entire thickness of the aquifer per unit time under unit groundwater gradient. Storativity measures the aquifer potential for water release by pressure decrease and aquifer compression, defined as the volume of water released from storage per unit surface area of aquifer per unit decline in hydraulic head. Specific yield measures unconfined aquifer potential for water release by gravity drainage; it is defined as the volume of water released from storage in an unconfined aquifer per unit aquifer volume. The Neuman delayed yield factor measures the effect of delayed yield from vertical gravity drainage and is related to the ratio of vertical hydraulic conductivity to horizontal hydraulic conductivity (K_Z/K_r), defined as follows (Neuman 1975):

$$\frac{K_Z}{K_r} = b\,\frac{b^2}{r^2} \qquad (5\text{-}32)$$

where

β	=	Neuman delayed yield factor [dimensionless]
b	=	Saturated thickness of the aquifer [L]
r	=	Distance from the pumping well to the observation well [L]
K_Z	=	Vertical hydraulic conductivity of the aquifer [LT^{-1}]
K_r	=	Horizontal hydraulic conductivity of the aquifer [LT^{-1}]

5.3.5 Results and Discussion

Aquifer hydraulic parameters were calculated using the groundwater pumping test data analysis software package AQTESOLV™ (Duffield and Rumbaugh 1991; HydroSOLVE 1996). The Neuman delayed yield model for partially penetrating wells in unconfined aquifers was selected to analyze the groundwater drawdown data corrected for tidal influence. Log-log plots of drawdown versus time were prepared, and the plots were matched visually with the Neuman type curves. The automatic matching option (using the least-square computational approach) offered by AQTESOLV™ was not used because the computational method is insensitive to the early data match and biased toward the data in the late stage of the test. The late data may include more errors caused by tidal influence and tidal correction. In addition, early data matched to Neuman's type curve A is important for accurate estimation of aquifer hydraulic parameters.

Figures 5-25 through 5-32 show the drawdown plots and the Neuman type curve matching for the various observation wells. As shown in the figures, the Neuman delayed yield type curves match well with the corrected drawdown plots. The drawdown data clearly illustrate the delayed gravity drainage effects. The curve matches in these figures indicate that the aquifer parameter calculation based on the pumping test data is representative.

Table 5-7 presents the results of the aquifer hydraulic parameter calculation using AQTESOLV™. The calculated aquifer hydraulic parameters are summarized as follows:

- The calculated aquifer transmissivity ranges from approximately 2,200 to 2,780 ft^2/day. The aquifer hydraulic conductivity was calculated based on the saturated aquifer thickness of 88 feet, ranging from 25 to 32 feet per day (ft/day) or 0.009 to 0.011 cm/sec. The range of the estimated hydraulic conductivity is typical for fine sand, which is consistent with the aquifer's lithologic conditions at the site.

- The estimated aquifer storativity ranges from approximately 0.001 to 0.008. In the Neuman delayed yield model, storativity represents the elastic release of water from the aquifer matrix at an early stage of the pumping test.

- Specific yield of the testing aquifer ranges from 0.02 to 0.12, approximately one to two orders of magnitude greater than the storativity values. The estimated specific yield values are within the typical range for unconfined aquifers.

- The estimated ratio of vertical to horizontal hydraulic conductivity ranges from 0.08 to 0.3. The ratios were calculated from the Newman delayed yield factor based on equation 5-32. The calculated ratios indicate the aquifer is considerably anisotropic in the vertical direction.

Generally, the estimated aquifer hydraulic conductivity values may represent the average horizontal properties of the testing aquifer. The hydraulic conductivity values calculated from data for the observation wells near the pumping well may be more representative of the upper zone condition. The calculated transmissivity, storativity and specific yield values are relatively constant for various depths of screened intervals and different distances from the pumping well, showing that the hydraulic property of the aquifer is relatively homogeneous.

5.4 DETERMINATION OF GROUNDWATER FLOW PATTERNS

Previous site investigations indicate that groundwater generally flows west in the vicinity of the NoVOCs™well. However, the mean groundwater flow direction and the horizontal and vertical

hydraulic gradients have not been adequately characterized in those investigations because tidal effects and variable groundwater densities caused by sea water intrusion were not considered. This section discusses the principles, procedures, and results of groundwater flow pattern determination, including mean groundwater level calculation from tidally influenced water levels and density correction for groundwater hydraulic gradient.

5.4.1 Mean Groundwater Level Calculation from Tidally Influence Water Levels

One widely applied method to calculate mean groundwater elevation from tidally influenced water levels was developed by Serfes (1991). The Serfes method is a three-step filtering approach (calculating moving averages) that uses hourly groundwater level data collected during a 70-hour period. The three-step filtering approach provides more accurate average groundwater levels than the straight arithmetic mean. The Serfes method was modified as explained below because water level data unaffected by aquifer testing for 70-hour periods were not available. The periods of data unaffected by pumping tests ranged from 30 to 62 hours. Also, the Serfes method was modified to allow the use of data collected more frequently than the 1-hour interval specified by Serfes (1991). Water levels were monitored at 20-minute intervals for the upper aquifer zone wells and at 15-second intervals for some of the lower aquifer zone wells.

The modified method is based on an average period of approximately 25 hours for a complete tidal cycle consisting of two high tides and two low tides. The procedures for the modified method for data of 20-minute frequency are as follows:

1. For a 50- to 75-hour groundwater elevation data series $\{H_i,\ i = 1, 2, \ldots, n\}$ with $149 \le n \le 224$, compute the first sequence of means $\{X_j,\ j = 1, 2, \ldots, n\text{-}74\}$ as follows:

$$X_j = \frac{1}{75}\sum_{m=0}^{74} H_{m+j} \quad where\ j = 1,2,\ldots,n-74 \qquad (5\text{-}33)$$

where

X_j = The first sequence of means [L]

H_{m+j} = Groundwater elevation data in 20-minute interval [L]

2. Then, the second sequence of means $\{Y_k\}$ $\{k=1,2, \ldots, n\text{-}142\}$ is calculated as follows:

$$Y_k = \frac{1}{75}\sum_{m=0}^{74} X_{m+k} \quad where \;\; k = 1,2,\ldots,n-148 \qquad (5\text{-}34)$$

where

Y_k = The second sequence of means [L]

X_{m+k} = The first sequence of means [L]

3. Finally, the mean groundwater elevation M is calculated as follows:

$$M = \frac{1}{n-148}\sum_{k=1}^{n-148} Y_k \qquad (5\text{-}35)$$

where

M = The mean groundwater elevation [L]

The mean groundwater elevations for wells MW-45, MW-47, and the upper screen of the NoVOCs™well were calculated using an electronic spreadsheet following the procedures above. Groundwater level data for wells MW-48, MW-49, MW-52, and MW-53 were recorded in 15-second intervals; therefore, calculation procedures for the mean elevation were further modified to use all the data that had been collected. The principle of this modification is the same as discussed above.

The mean groundwater elevations calculated for wells MW-45, MW-48, MW-52, and the upper screen of the NoVOCs™well represent groundwater flow patterns in the upper aquifer zone. The mean groundwater flow direction in the lower aquifer zone was characterized by the mean water elevation data from wells MW-47, MW-49, and MW-53. Data for other monitoring wells were not used because the wells were either constructed between the two zones or fully penetrate the aquifer. Groundwater elevation data for some of the wells are not available.

5.4.2 Density Correction of Groundwater Levels

Evaluation of groundwater flow pattern in the vicinity of the NoVOCs™well is further complicated by seawater intrusion. The salinity of groundwater at the site is generally 2 to 3 percent and the density of groundwater samples from almost all the monitoring wells is greater than 1 gram/cubic centimeter (g/cm^3). In addition, groundwater density varies by well location and depth. In general, the density of

groundwater is higher in the lower aquifer zone. In the following sections, the calculation of equivalent fresh-water heads and the correction of groundwater levels measured by pressure transducers are discussed.

5.4.2.1 Calculation of Equivalent Fresh-Water Heads

Calculation of equivalent fresh-water heads (elevations) from an aquifer with variable water density is the first step of the density correction. Equivalent fresh-water heads plotted on maps and contoured are necessary to estimate horizontal groundwater flow direction and hydraulic gradient. The apparent head measurements in a density-variable aquifer should not be used to plot groundwater level contour maps: the contours of such plots will be misleading because the density effect can cause water to flow from apparent low to apparent high heads.

The following discussion presents the principles and procedures for calculating the equivalent fresh-water head. Density correction procedures for data collected by pressure transducer are different from those for manual measurements using water level indicators.

Groundwater hydraulic head is a sum of elevation head and pressure head, described as follows (Freeze and Cherry 1979):

$$h = z + y \qquad (5\text{-}36)$$

where

h	=	The hydraulic head [L]
z	=	Elevation of the point of measurement [L]
Ψ	=	The pressure head [L]

The pressure head of groundwater is a function of gage pressure and groundwater density; therefore, the hydraulic head can be further defined as follows:

$$h = z + \frac{p}{rg} \qquad (5\text{-}37)$$

where

p	=	Groundwater gage pressure [$ML^{-1}T^{-2}$]
ρ	=	Groundwater density [ML^{-3}]
g	=	Gravitational acceleration [LT^{-2}]

Equation 5-37 shows that the hydraulic head (h) for higher density water will be less than the hydraulic head for fresh water under the same pressure and elevation conditions. Groundwater does not necessarily flow from the higher head to the lower head under this circumstance.

From Equation 5-37, the measured groundwater elevation above the MLLW in a monitoring well at the site is as follows:

$$h = z + \frac{p}{r_b g} \qquad (5\text{-}38)$$

where

h	=	The measured groundwater elevation using water level indicator [L]
ρ_b	=	Density of groundwater in the well [ML^{-3}]
z	=	Elevation of the middle point of the well screen above (positive) or below (negative) a datum [L]
p	=	Groundwater gage pressure at the middle point of the well screen [$ML^{-1}T^{-2}$]

Also from Equation 5-37, the equivalent fresh-water head above the datum in the monitoring well is given by:

$$h^* = z + \frac{p}{r_0 g} \qquad (5\text{-}39)$$

where

h^*	=	Equivalent fresh water head above the datum [L]
ρ_0	=	Density of fresh water (assumed to be 1) [ML^{-3}]

Considering that the gage pressure of groundwater in the well is constant, Equations 5-38 and 5-39 can be combined to obtain the following equation:

$$(h^* - z)\rho_0 g = (h - z)\rho_b g \qquad (5\text{-}40)$$

Rearranging Equation 5-40 and substituting specific gravity $\gamma = \rho_b/\rho_0$ into the equation, the equivalent fresh-water head, h^*, is defined as follows:

$$h^* = \gamma h + (1-\gamma)z \qquad (5\text{-}41)$$

where

γ = Specific gravity of the groundwater [dimensionless]

Equation 5-41 should be used to calculate equivalent fresh-water head based on the water level measurements collected manually by water level indicators. Equation 5-41 may be used for pressure transducer data under certain circumstances, as explained in the next section.

5.4.2.2 Correction of Groundwater Levels Measured by Pressure Transducer

Pressure transducers measure water pressure. The water pressure reading is usually converted by data logger software to a water head above the transducer. The conversion is usually based on the density of fresh water (Equation 5-39). If the water density differs from that of fresh water but the conversion is based on fresh water, the resulting water head value will be the fresh water equivalent head relative to the transducer. If the conversion is based on the actual density of the water (Equation 5-38), the resulting water head value will be the actual water head relative to the transducer. Correcting pressure transducer data for density effects depends on whether raw pressure data were converted to heads using fresh water density or actual water density. Correcting the data also depends on (1) the manner in which the data logger software processes the data, (2) whether initial water levels input into the data logger have been corrected for density effects, and (3) whether multiple manual water level measurements are available for the data recording period. Several cases of data handling are discussed below (data logger configurations are described in bold, followed by an explanation of corrections that should be applied):

- **Case 1: The actual density of the groundwater was measured and the data logger used actual density to convert pressure data to water head above the transducer. The initial water level, measured manually and input into the data logger, was not corrected for density effects.**

All water levels recorded by the data logger are actual water levels and not fresh-water equivalent water levels. Equation 5-41 should be used to convert all water level data output from the data logger.

- **Case 2: The actual density of the groundwater was measured. The initial water level (manually measured) was corrected to a fresh-water equivalent using Equation 5-41 and input into the data logger. The data logger used fresh-water density to convert pressure to fresh-water equivalent head above the transducer. The data logger was set up to record changes from the initial water level.**

  No additional density correction is required. All data logger output will be fresh-water equivalent water levels.

- **Case 3: Actual density of groundwater was not considered in the data logger configuration. Multiple manual measurements of water levels were collected during the recording period.**

  Using the manual measurements, which represent the apparent groundwater elevations, the pressure transducer data should be adjusted to also represent apparent groundwater elevations. Equation 5-41 can then be applied to the entire adjusted data set to obtain equivalent fresh-water elevations.

- **Case 4: Actual density of groundwater was not considered in the data logger configuration. Only initial manual measurement of water levels was collected during the recording period.**

  The change in water level from the initial data point should be calculated for each pressure transducer data point. The initial pressure transducer data point should be adjusted to represent the apparent water level elevation based on the initial manual water level measurement. Equation 5-41 should be applied to the adjusted initial groundwater elevation to obtain the initial fresh-water equivalent elevation. No density correction is needed for the water-level changes calculated from the pressure transducer data. The water-level changes should be directly added to or subtracted from the density-corrected initial groundwater elevation to obtain fresh-water equivalent elevations for the entire data set.

5.4.3 Corrected Water Levels and Horizontal Groundwater Flow Direction

Groundwater elevations and drawdown changes were measured using pressure transducers during the various phases of the aquifer tests. Manual water level measurements were also collected at the pumping well and at most observation wells during the tests. The data were corrected following the procedures specified for the Case 3 and Case 4 examples discussed in the previous section. The corrected results are presented in Appendixes C through G.

Static groundwater levels were corrected for tidal influence following the procedures discussed in Section 5.4.1. Mean groundwater elevations for the upper aquifer zone were calculated using the upper screen of NoVOCs™ well and the three upper zone NoVOCs™ observation wells (MW-45, MW-48, and MW-52). Mean groundwater elevations for the lower aquifer zone were calculated using the three lower zone NoVOCs™ observation wells (MW-47, MW-49, and MW-53). The mean groundwater elevations after tidal correction are listed in Table 5-8.

The equivalent fresh-water heads of the mean groundwater elevations were calculated following the procedures discussed in Section 5.4.2. The first step of the calculation is to obtain density data for various monitoring well locations and aquifer depths because the groundwater density was not directly measured. Jacobs Engineering Group, Inc. (1995b) applied an empirical equation developed by de Marsily (1986) to calculate groundwater density from total dissolved solids (TDS) data. The empirical equation was developed based on a laboratory test with sodium chloride solution and a linear regression analysis.

The empirical equation developed by de Marsily (1986) is as follows:

$$r = \left(6.87 \times 10^{-4} \, C_{TDS} \right) + 998.4575 \qquad (5\text{-}42)$$

where

ρ	=	Groundwater density (kg/m^3)
C_{TDS}	=	TDS concentration (mg/L)

The groundwater density and results for equivalent fresh-water head calculation are presented in Table 5-8.

The mean equivalent fresh-water head contours for the upper aquifer zone are plotted in Figures 5-33 and 5-34. Figure 5-33 is based on four points (including data for well MW-48), and Figure 5-34 is based on three points (excluding data for well MW-48). The two presentations (with and without data for well MW-48 data) are provided because the screen of well MW-48 is at a lower elevation than in the other three wells used to construct the contours. The mean equivalent fresh-water head contours for the lower aquifer zone are plotted in Figure 5-35. These contour maps represent the mean static water levels and flow directions with tidal and pumping influences removed. Effects caused by variation in groundwater

density variation were also corrected. These contour maps are considered representative of the natural groundwater flow pattern.

As shown in Figures 5-33, 5-34, and 5-35, groundwater generally flows to the west or northwest in both of the upper and lower aquifer zones. The horizontal hydraulic gradient in both aquifer zones is relatively flat, ranging from 0.005 to 0.01 feet per feet in the upper zone and approximately 0.006 in the lower zone. Data for generating the contour maps were limited (four points for the upper aquifer zone and three points for the lower aquifer zone) because other NoVOCs™ observation wells were completed at depths between the two aquifer zones. Also, data were not available for some of the observation wells because of data logger malfunction.

5.4.4 Vertical Hydraulic Gradient Correction

Calculation of vertical hydraulic gradient in a fresh-water aquifer (groundwater density of 1 g/cm^3) is simple: for two vertically aligned wells, the vertical hydraulic gradient equals the head difference between the wells divided by the distance between the midpoint of the well screen intervals. However, calculation of vertical hydraulic gradient in a density-variable aquifer is relatively complex. Incorrect calculations of the vertical hydraulic gradient by simply using equivalent fresh-water heads to determine the head difference are common. The vertical hydraulic gradient in a density-variable aquifer is a function of the equivalent fresh-water heads, the distance between the two intervals, and the groundwater density. This section discusses the principles and the reason for calculating vertical hydraulic gradient differently from the horizontal hydraulic gradient. The procedures to calculate the vertical hydraulic gradient in a density-variable aquifer are also presented.

Vertical hydraulic gradient is not calculated in this report because limited groundwater density data are available. Also, vertical hydraulic gradient was not identified as a key parameter in the pumping test data analysis and NoVOCs™ well evaluation. The equations and procedures discussed in this section can be followed in future data analysis for the vertical hydraulic gradient at the site.

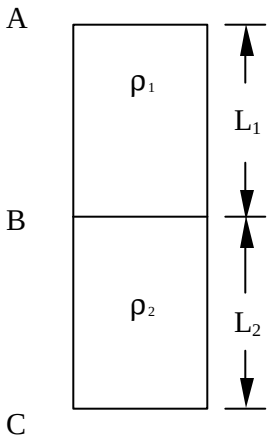

Considering water column ABC filled with a porous medium as shown in the Drawing: the upper portion, AB, has a height L_1 and contains water (or any fluid) with a density equal to ρ_1; the lower portion, BC, has a height of L_2 and contains water with a density equal to ρ_2. Water in the column is assumed to be in a hydraulic steady state, that is, no vertical flow occurs. Vertical hydraulic gradient is to zero between any two points within the column. Also, it is assumed that no density-driven flow and no density diffusion occur across the boundary line B.

If the bottom of the column is set at the datum, that is, the elevation z equals zero at point C, from Equation 5-39, the equivalent fresh water-head at the three points (A, B, and C) will be given as:

$$h_A^* = z_A + \frac{p_A}{r_0 g} \qquad (5\text{-}43)$$

$$h_B^* = z_B + \frac{p_B}{r_0 g} \qquad (5\text{-}44)$$

$$h_C^* = z_C + \frac{p_C}{r_0 g} \qquad (5\text{-}45)$$

where

p_A, p_B, and p_C = The groundwater pressure gages at points A, B, and C

z_A, z_B, and z_C = The elevations of points A, B, and C

Equations 5-43, 5-44, and 5-45 can be solved as follows, considering $p_A=0$, $p_B=\rho_1 g L_1$, $p_C=\rho_1 g L_1+\rho_2 g L_2$, $z_A=L_1+L_2$, $z_B=L_2$, and $z_C=0$:

$$h_A^* = (L_1 + L_2) + 0 = L_1 + L_2 \qquad (5\text{-}46)$$

$$h_B^* = L_2 + \frac{r_1 g L_1}{r_0 g} = g_1 L_1 + L_2 \qquad (5\text{-}47)$$

$$h_C^* = 0 + \frac{(r_1 L_1 + r_2 L_2) g}{r_0 g} = g_1 L_1 + g_2 L_2 \qquad (5\text{-}48)$$

Because $\gamma_1 \neq \gamma_2 \neq 1$, Equation 5-46, 5-47, and 5-48 show that the equivalent fresh-water heads at the three points are not equal. This result contradicts the assumption that no vertical flow occurs in the water column. Therefore, the difference in the two equivalent fresh-water heads divided by the distance between the two points does not equal the vertical hydraulic gradient in aquifers with variable density groundwater.

In general, the vertical hydraulic gradient between two vertically aligned points within variable density groundwater equals the difference of the fresh-water equivalent heads at the two points divided by the distance plus a constant. That is:

$$I_{AB} = \frac{h_A^* - h_B^*}{L_1} + C_1 \qquad (5\text{-}49)$$

$$I_{BC} = \frac{h_B^* - h_C^*}{L_2} + C_2 \qquad (5\text{-}50)$$

$$I_{AC} = \frac{h_A^* - h_C^*}{L_1 + L_2} + C_3 \qquad (5\text{-}51)$$

where

I_{AB} = Vertical hydraulic gradient between points A and B.

I_{BC} = Vertical hydraulic gradient between points B and C.

I_{AC} = Vertical hydraulic gradient between points A and C.

From Equations 5-46, 5-47, and 5-48, considering $I_{AB} = I_{BC} = I_{AC} = 0$, for steady state condition, we can solve C_1, C_2 and C_3 as:

$$C_1 = \frac{h_B^* - h_A^*}{L_1} = \frac{g_1 L_1 + L_2 - (L_1 + L_2)}{L_1} = g_1 - 1 \quad (5\text{-}52)$$

$$C_2 = \frac{h_C^* - h_B^*}{L_2} = \frac{g_1 L_1 + g_2 L_2 - (g_1 L_1 + L_2)}{L_2} = g_2 - 1 \quad (5\text{-}53)$$

$$C_3 = \frac{h_C^* - h_A^*}{L_1 + L_2} = \frac{g_1 L_1 + g_2 L_2 - (L_1 + L_2)}{L_1 + L_2} = \frac{g_1 L_1 + g_2 L_2}{L_1 + L_2} - 1 \quad (5\text{-}54)$$

Therefore, vertical hydraulic gradient between any two points in an aquifer with density-variable groundwater can be calculated using the following general equation (based on Equations 5-49 through 5-54):

$$I_V = \frac{h_u^* - h_l^*}{l} + (g - 1) \quad (5\text{-}55)$$

where

I_V = Vertical hydraulic gradient between two vertically aligned points within the aquifer (positive value represents downward gradient) [dimensionless]

h_u, h_l = The equivalent fresh water heads at the two points (higher elevation and lower elevation points, respectively) [L]

l = Vertical distance between the two points [L]

γ = Specific gravity of groundwater between the two points [dimensionless]

The specific gravity of groundwater between the two points should be carefully chosen when Equation 5-55 is used. If the groundwater density is not constant between the upper and lower aquifer zones, a thickness-weighted average of the specific gravity for multiple density strata should be used. The weighted average of the specific gravity is calculated as follows:

$$g = \frac{\sum_{i=1}^{n} g_i l_i}{\sum_{i=1}^{n} l_i}, \qquad i = 1,2,\ldots n \qquad (5\text{-}56)$$

where

γ = The weighted average of the specific gravity of groundwater

γ_i = The specific gravity of the i^{th} strata

l_i = The thickness of the i^{th} strata

5.5 DIPOLE FLOW TEST

The dipole flow test (DFT), a new single-well hydraulic test for aquifer characterization, was first proposed by Kabala (1993). The test was designed to characterize the vertical distribution of local horizontal and vertical hydraulic conductivities near the test well. Measures of the aquifer's anisotropy ratio and storativity can also be obtained through DFT data analysis. DFT is a cost-effective method for aquifer hydraulic characterization because (1) the test duration is short; the test generally lasts no more than a few hours, and (2) no investigation-derived waste is generated because the water from the pumping chamber is injected to the aquifer through recharge chamber.

5.5.1 Mathematical Models

Kabala (1993) presented a mathematical model describing drawdown (or water level rise) during a dipole flow test in each of the isolated chambers of a well situated in a leaky homogeneous anisotropic aquifer. Major assumptions for this original model are:

- The aquifer is homogeneous and anisotropic and horizontally situated
- The aquifer is under either leaky or confined conditions
- The test well fully penetrates the aquifer thickness
- Water is removed through one of the two open screened intervals and discharged to another interval instantaneously
- Linear vertical head distribution is assumed in the semiconfining layer (leaky aquitard)

- Water storage in the leaky aquitard is negligible
- Flows in the aquifer zones are mainly horizontal, but primarily vertical mithin the leaky aquitard
- Well bore storage and well losses are insignificant
- "Skin effect" (short-circuiting through the sand packs) is negligible

The analytical solutions for drawdown in the pumping chamber and water level rise in the recharge chamber are presented by Kabala (1993). The transient solution describing drawdown is given as follows:

$$s(t) = \frac{Q}{4pK_r b}\left\{W(u_r; b_w) + \frac{2b^2}{4p^2\Delta^2}\sum_{n=1}^{\infty}\frac{1}{n^2}[\sin\frac{np(d+2\Delta)}{b} - \sin\frac{npd}{b}]^2\, W[u_r; (b_w{}^2 + \frac{(npr_w)^2}{a^2b^2})^{1/2}]\right\} \quad (5\text{-}57)$$

where

s(t)	=	Drawdown in the pumping chamber [L]
t	=	Time since beginning of the test [L]
Q	=	Pumping rate [L^3T^{-1}]
K_r	=	Horizontal hydraulic conductivity [LT^{-1}]
b	=	Aquifer thickness [L]
d	=	Distance from the top of aquifer to the top of the upper chamber [L]
Δ	=	Half of the length of the screen interval [L]
a^2	=	Aquifer anisotropy ratio, defined as K_r/K_z [dimensionless]
$W(u_r, \beta_w)$ =		Leaky aquifer well function, defined as:

$$W(u_r; b_w) = \int_{u_r}^{\infty}\frac{1}{y}\exp(-y - \frac{b_w{}^2}{4y})dy \quad (5\text{-}58)$$

where

u_r	=	Dimensionless time, defined as: $r_w{}^2 S_s/4K_r t$
β_w	=	Leaky factor defined as: $r_w/(K_r bb'/K')^{1/2}$
r_w	=	Radius of the well casing [L]
S_s	=	Aquifer specific storage [L^{-1}]

b' = Aquitard (semi-confining layer) thickness [L]

K' = Aquitard vertical hydraulic conductivity [LT^{-1}]

A similar solution can be derived to describe water level rise due to injection in the recharge chamber with a negative pumping rate. Combining the pumping and injection effects, the actual drawdown in the pumping chamber is given by:

$$s(t) = \frac{Q}{pK_r b}\sum_{n=1}^{\infty}[\frac{\sin(np\Delta / b)}{np\Delta / b}]^2 \cdot \sin(np\frac{l+d}{2b})\sin(np\frac{l-d-2\Delta}{2b})\cos(np\frac{d+\Delta}{b})\cdot W[u_r;(b_w{}^2 + \frac{(npr_w)^2}{a^2b^2})^{1/2}] \qquad (5\text{-}59)$$

The solution for actual water level rise in the recharge chamber is given by:

$$s(t) = \frac{Q}{pK_r b}\sum_{n=1}^{\infty}[\frac{\sin(np\Delta / b)}{np\Delta / b}]^2 \cdot \sin(np\frac{l+d}{2b})\sin(np\frac{l-d-2\Delta}{2b})\cos(np\frac{l-\Delta}{b})\cdot W[u_r;(b_w{}^2 + \frac{(npr_w)^2}{a^2b^2})^{1/2}] \qquad (5\text{-}60)$$

Equations (5-59) and (5-60) are the transient solutions for the dipole flow test. The steady state solution for drawdown in the pumping chamber is as follows:

$$s(t) = \frac{2Q}{pK_r b}\sum_{n=1}^{\infty}[\frac{\sin(np\Delta / b)}{np\Delta / b}]^2 \cdot \sin(np\frac{l+d}{2b})\sin(np\frac{l-d-2\Delta}{2b})\cos(np\frac{d+\Delta}{b})\cdot K_0[(b_w{}^2 + \frac{(npr_w)^2}{a^2b^2})^{1/2}] \qquad (5\text{-}61)$$

Where

K_0 = Zero-order modified Bessel function of the second kind,

l = Distance from the top of the aquifer to the bottom of the lower screen.

5.5.2 Modified Dipole Flow Test Solution for Wellbore Storage

Kabala (1998) developed a new DFT model to account for wellbore storage effects in the pumping and injection chambers. In the wellbore storage DFT model, measured drawdown (or water level rise) is the

sum of aquifer drawdown and wellbore storage drawdown. Dimensionless wellbore storage parameters for the pumping and recharge chambers are defined as:

$$C_{PD} = \frac{(r_i / r_w)^2}{4S} \tag{5-62}$$

$$C_{RD} = \frac{1 - (r_i / r_w)^2}{4S} \tag{5-63}$$

where

C_{PD}	=	Dimensionless wellbore storage parameter for the pumping chamber
C_{RD}	=	Dimensionless wellbore storage parameter for the recharge chamber
r_i	=	Radius of inner well casing (eductor pipe)[L]
r_w	=	Radius of well casing [L]
S	=	Aquifer storativity or specific yield [dimensionless]

Laplace transformation is used to solve the partial differential equations that describe drawdown (or water level rise) in the pumping (or recharge) chamber during the DFT where the wellbore storage effect is considered. The drawdown in the pumping chamber s_{pump} can be described as:

$$s_{pump}(p) = s_{pp}(p) + s_{pi}(p) \tag{5-64}$$

where p is the Laplace transformation variable, s_{pp} (p) is the drawdown caused by pumping, and s_{pi} (p) is the water level caused by injection (expressed as negative drawdown). The two components of the water level response are defined as follows:

$$s_{pp}(p) = \frac{Q}{4pK_r b} \cdot \frac{\frac{2}{p} K_0(\sqrt{p}) + 4\sum_{n=1}^{\infty} \frac{a_n^{\,2}}{p} K_0(\sqrt{p + g_n^{\,2}})}{C_{PD} p^2 [\frac{2}{p} K_0(\sqrt{p}) + 4\sum_{n=1}^{\infty} \frac{a_n^{\,2}}{p} K_0(\sqrt{p + g_n^{\,2}})] + 1} \tag{5-65}$$

and

$$s_{pi}(p) = \frac{-Q}{4pK_r b}$$

$$\cdot \left\{1 - \frac{[\frac{2}{p}K_0(\sqrt{p}) + 4\sum_{n=1}^{\infty}\frac{b_n^{\,2}}{p}K_0(\sqrt{p+g_n^{\,2}})][\frac{2}{p}K_0(\sqrt{p}) + 4\sum_{n=1}^{\infty}\frac{a_n^{\,2}b_n^{\,2}}{p}K_0(\sqrt{p+g_n^{\,2}})]}{C_{RD}p^2[\frac{2}{p}K_0(\sqrt{p}) + 4\sum_{n=1}^{\infty}\frac{b_n^{\,2}}{p}K_0(\sqrt{p+g_n^{\,2}})] + 1}\right\} \quad (5\text{-}66)$$

Variables α_n, β_n, and γ_n are defined as follows:

$$a_n = \frac{b}{np\Delta_u} \cdot \sin(\frac{np\Delta_u}{b}) \cdot \cos[\frac{np(d+\Delta_u)}{b}] \quad (5\text{-}67)$$

$$b_n = \frac{b}{np\Delta_l} \cdot \sin(\frac{np\Delta_l}{b}) \cdot \cos[\frac{np(l-\Delta_l)}{b}] \quad (5\text{-}68)$$

$$g_n = \frac{npr_w}{b\sqrt{K_r / K_z}} \quad (5\text{-}69)$$

where:

Δ_u = Half of the upper screened interval [L]

Δ_l = Half of the lower screened interval [L]

5.5.3 Dipole Flow Test Data Interpretation and Aquifer Anisotropy Estimation

The dimensionless drawdown in the pumping chamber versus dimensionless time can be plotted as groups of type curves with different anisotropy ratios ($a^2 = K_r/K_z$) and storativity (or specific yield) values. The type curves are generated by plotting dimensionless drawdown s_D versus dimensionless time τ, which are defined as follows:

$$s_D = \frac{s(t)}{s(\infty)} \quad (5\text{-}70)$$

and

$$t = \frac{n\,t}{r_w^{\,2}} \qquad (5\text{-}71)$$

where

$s(\infty)$	=	Steady state drawdown or water level rise during the DFT [L]
ν	=	Aquifer hydraulic diffusivity, defined as T/S or K_r/S_s [L^2T^{-1}]

Drawdown (or water level rise) data collected during the DFT then be normalized to dimensionless drawdown (or water level rise) with values ranging from 0 to 1, as follows:

$$s_D(t) = \frac{s(t+t_0) - s_{\min}}{s_{\max} - s_{\min}} \qquad (5\text{-}72)$$

where

$s_D(t)$	=	Normalized dimensionless drawdown (or water level rise)
$s(t+t_0)$	=	Drawdown (or water level rise) at time $t+t_0$ [L]
t_0	=	The beginning time of a given step of the DFT [T]
s_{max}	=	The maximum drawdown (or water level rise) during a given step of the DFT [L]
s_{min}	=	The minimum drawdown (or water level rise) during a given step of the DFT [L]

The normalized drawdown or water level rise versus time are plotted for the type curve match. A scale factor (A) is applied to the real-time plots. The scale factor is applied for two purposes: (1) transferring real time to dimensionless time so the horizontal axes of the type curves and test data are comparable, and (2) adjusting the horizontal positions of the data plots so that a best match to one of the type curves can be obtained. The scale factor is defined as:

$$A = \frac{n}{r_w^{\,2}} = \frac{K_r}{S_s r_w^{\,2}} \qquad (5\text{-}73)$$

From the type curve match, the aquifer anisotropy ratio is obtained from the value of parameter a^2 (which equals K_r/K_z). In addition, aquifer horizontal hydraulic conductivity can be calculated from the values of parameters S (or S_y), and A. The aquifer horizontal hydraulic conductivity K is calculated by the following equation:

$$K_r = \frac{A \cdot r_w^{\,2} S}{b} \qquad (5\text{-}74)$$

DFT data collected during Step 4 recovery in the recharge chamber were considered the most suitable for parameter estimation because the water level rise data were least affected by variations in pumping rate variations and head fluctuations.

Tidal influence during the DFT is removed using data collected from well MW-51. Comparison of water level data from the NoVOCs™ well and observation well MW-51 shows that the tidal fluctuations in the two wells are almost identical. Well MW-51 also had minimum impact from the DFT because of its distance from the NoVOCs™ well. The least-square algorithm was used to simulate the tidal fluctuations in the NoVOCs™ well. The drawdown (or water level rise) correction procedure is similar to the procedures presented in Section 5.1.

Figure 5-36 shows the recovery data plots and type curve match for the DFT Step 4 recharge chamber. The type curves are generated using the DFT model considering well bore storage. The group of the type curves in Figure 5-36 represents storativity S=0.01 and anisotropy ratios $a^2 = K_r/K_z$ = 100, 30, 10, 3, and 1. The normalized dimensionless DFT recovery data with time are represented by circles,whereas the normalized recovery data versus scaled time (dimensionless time) are plotted as thick dash line.

From the DFT recovery data plots and type curve match (Figure 5-36), the aquifer hydraulic parameters are estimated as: K_r = 0.0115 cm/sec, $0.001 \leq S \leq 0.01$, and K_r/K_z = 4.93. These results are very close to the parameter estimated by interpreting pumping test data (Section 5.3). The aquifer hydraulic parameters estimated through DFT are also presented in Table 5-7.

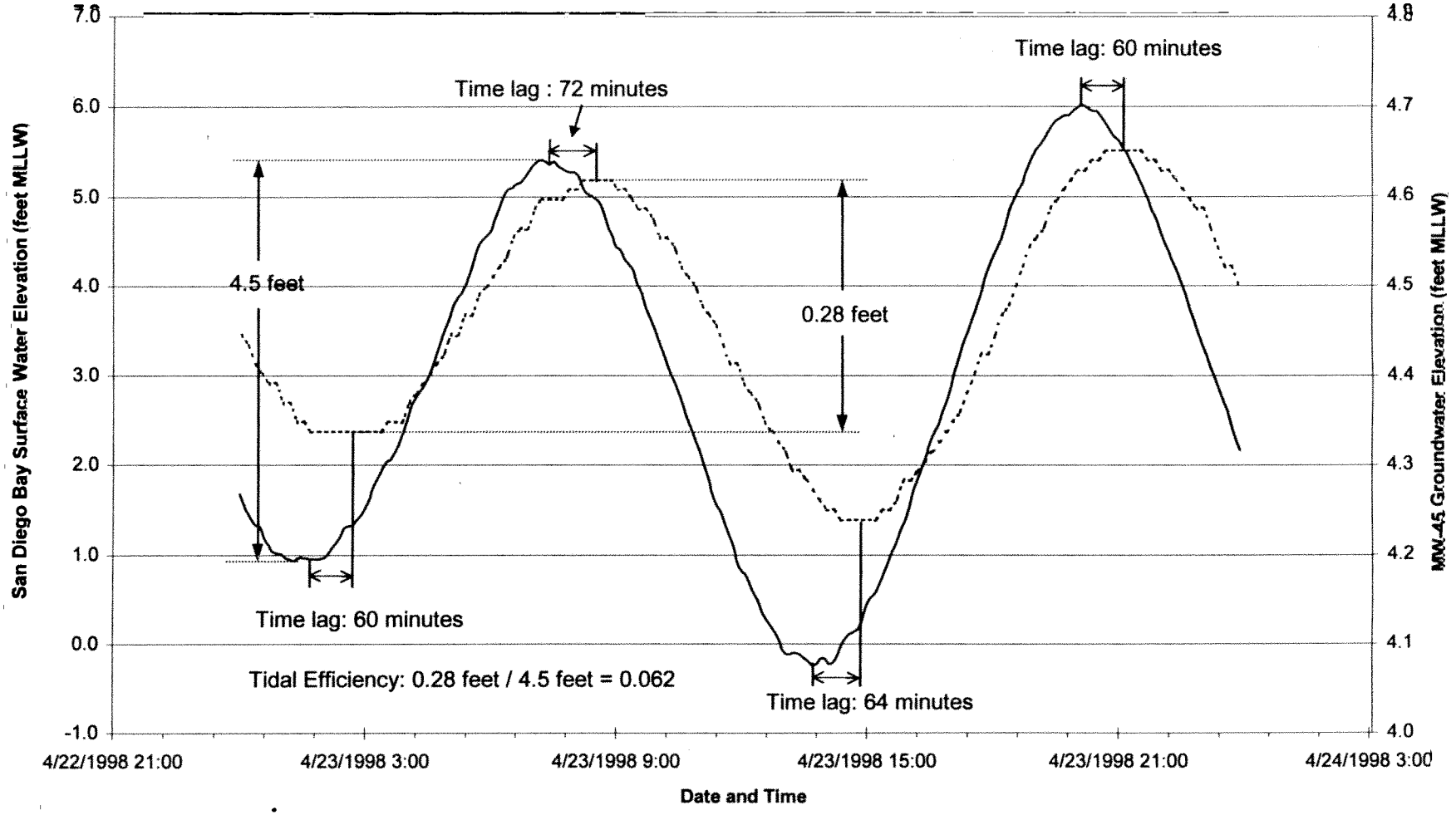

NAS NORTH ISLAND SITE 9
NoVOCs™ HYDROGEOLOGICAL INVESTIGATION

FIGURE 5-1
WATER LEVEL COMPARISON BETWEEN SAN DIEGO BAY AND OBSERVATION WELL MW45

Tetra Tech EM Inc.

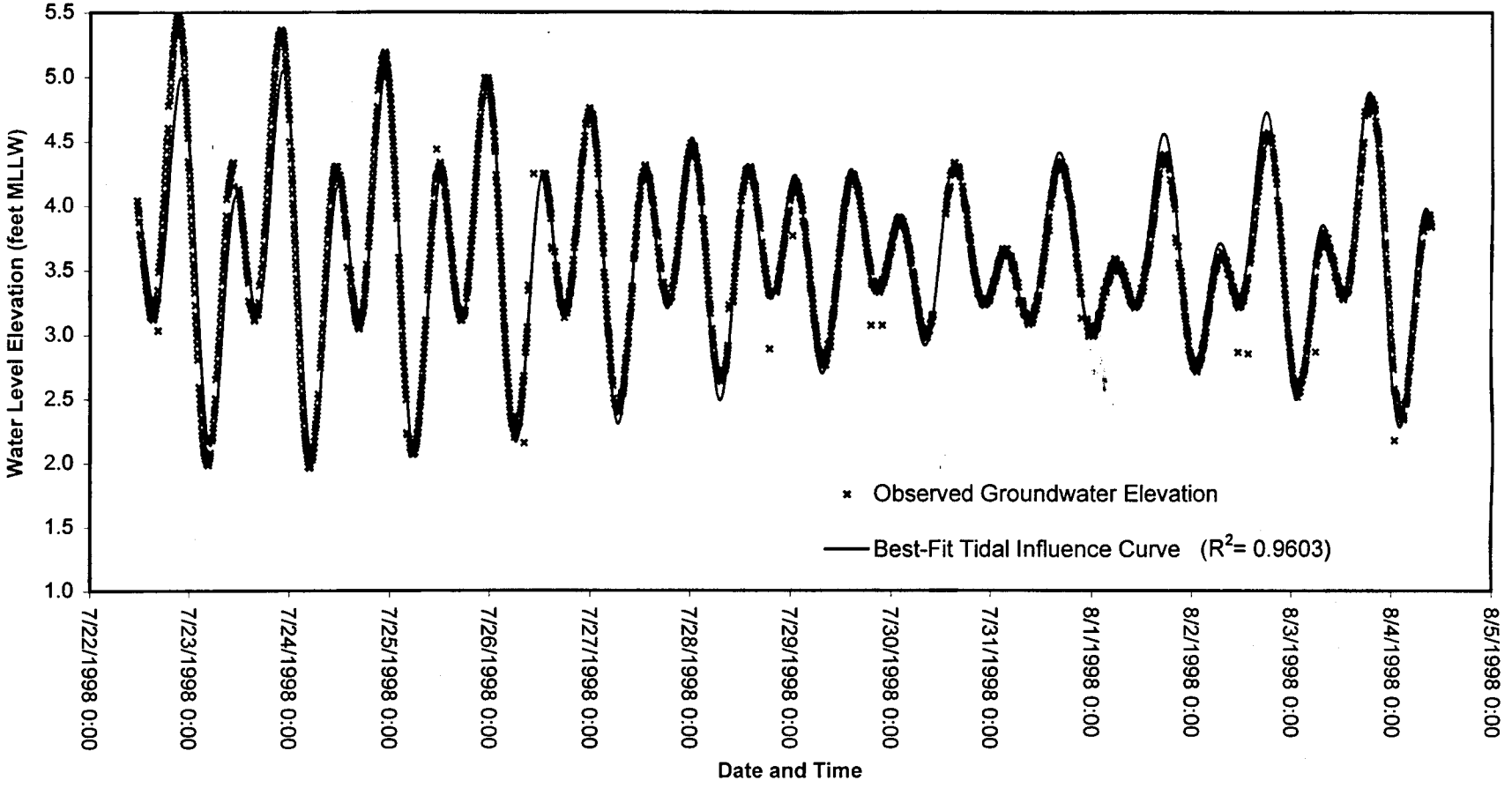

NAS NORTH ISLAND SITE 9
NoVOCs™ HYDROGEOLOGICAL INVESTIGATION

FIGURE 5-2
OBSERVED GROUNDWATER ELEVATION AND BEST-FIT TIDAL INFLUENCE CURVE FOR WELL MW20

Tetra Tech EM Inc.

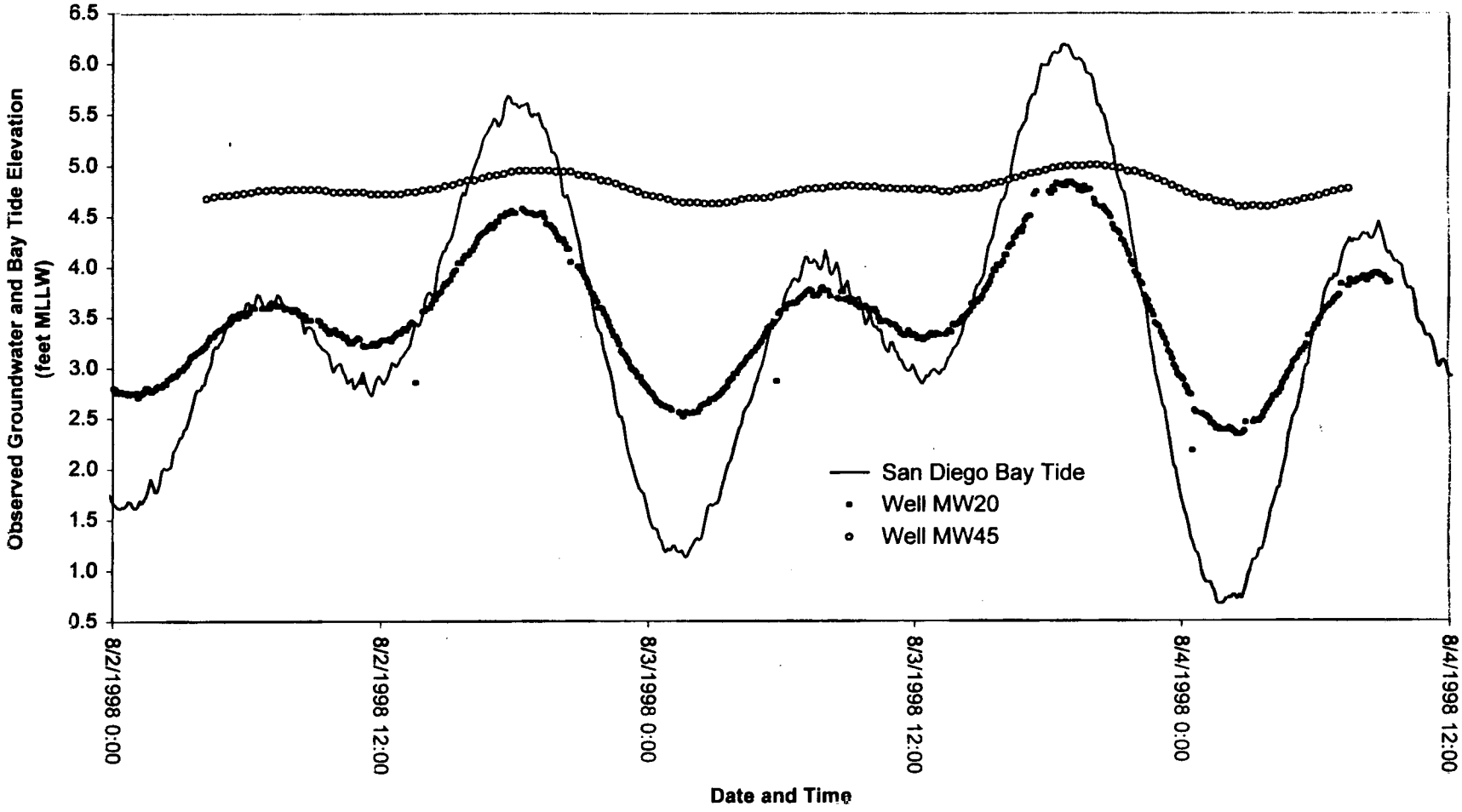

NAS NORTH ISLAND SITE 9
NoVOCs™ HYDROGEOLOGICAL INVESTIGATION

FIGURE 5-3
OBSERVED WATER LEVEL COMPARISON AMONG BAY TIDE, MW20 AND MW45

Tetra Tech EM Inc.

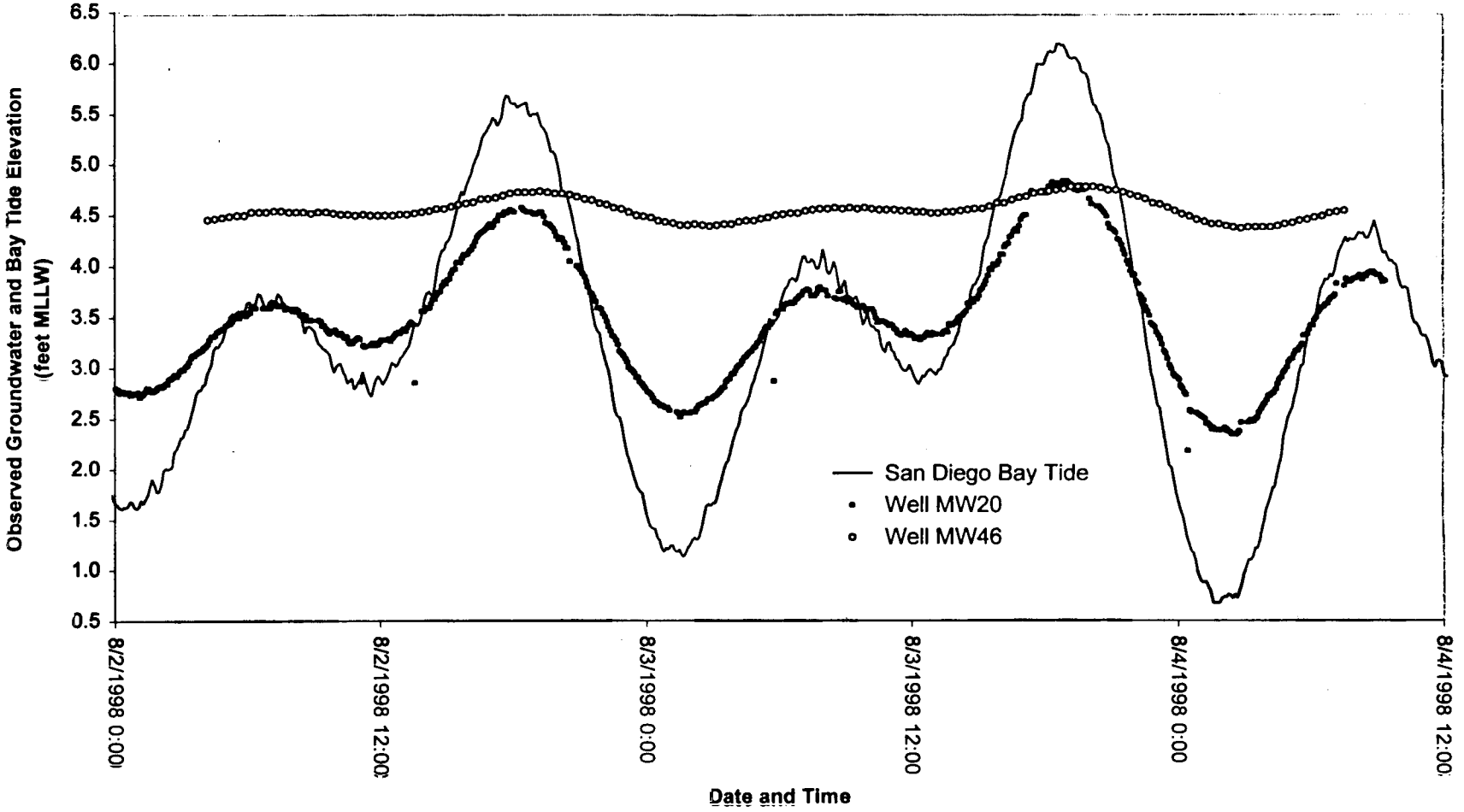

NAS NORTH ISLAND SITE 9
NoVOCs™ HYDROGEOLOGICAL INVESTIGATION

FIGURE 5-4
OBSERVED WATER LEVEL COMPARISON AMONG BAY TIDE, MW20 AND MW46

Tetra Tech EM Inc.

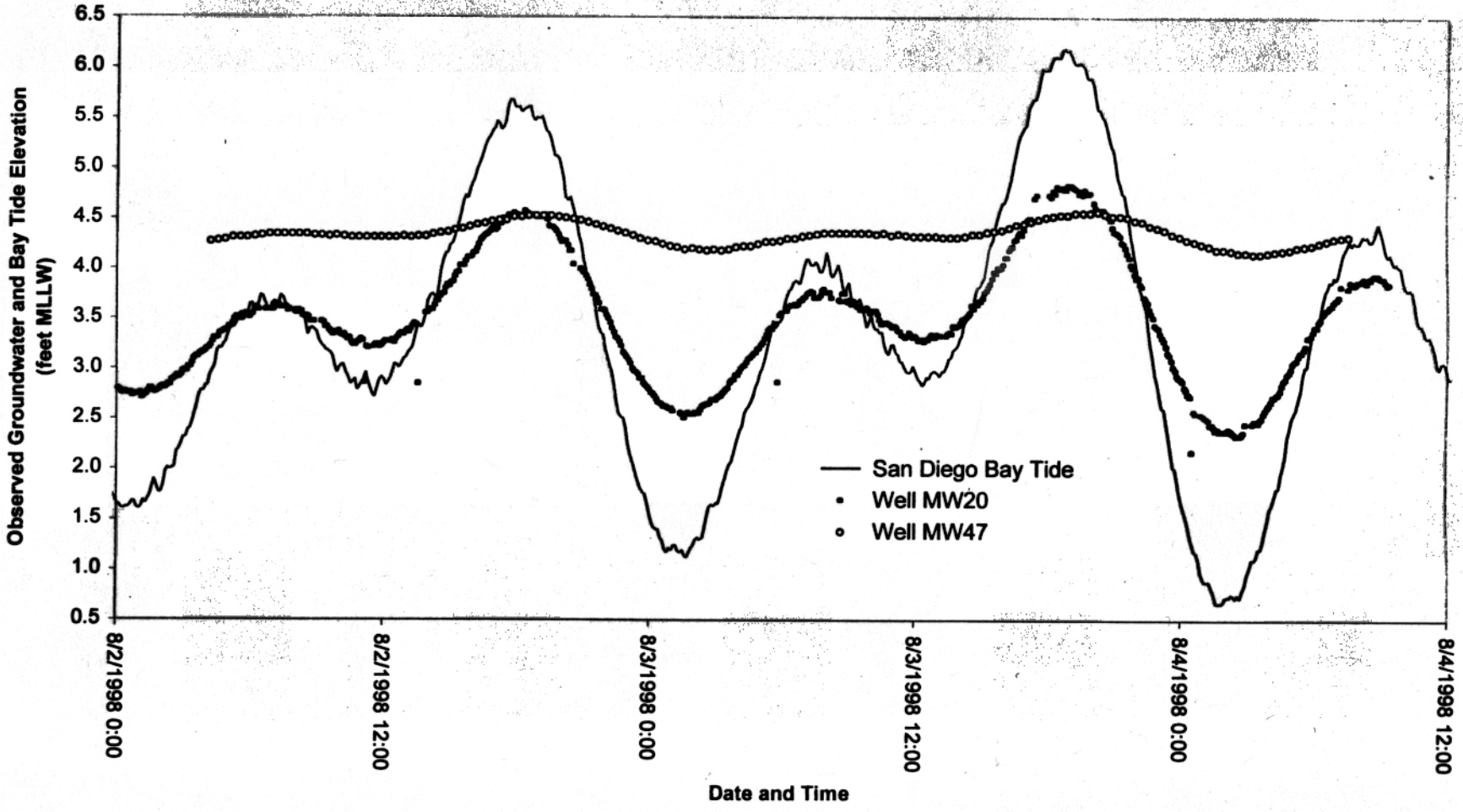

NAS NORTH ISLAND SITE 9
NoVOCs™ HYDROGEOLOGICAL INVESTIGATION

FIGURE 5-5
OBSERVED WATER LEVEL COMPARISON AMONG BAY TIDE, MW20 AND MW47

Tetra Tech EM Inc.

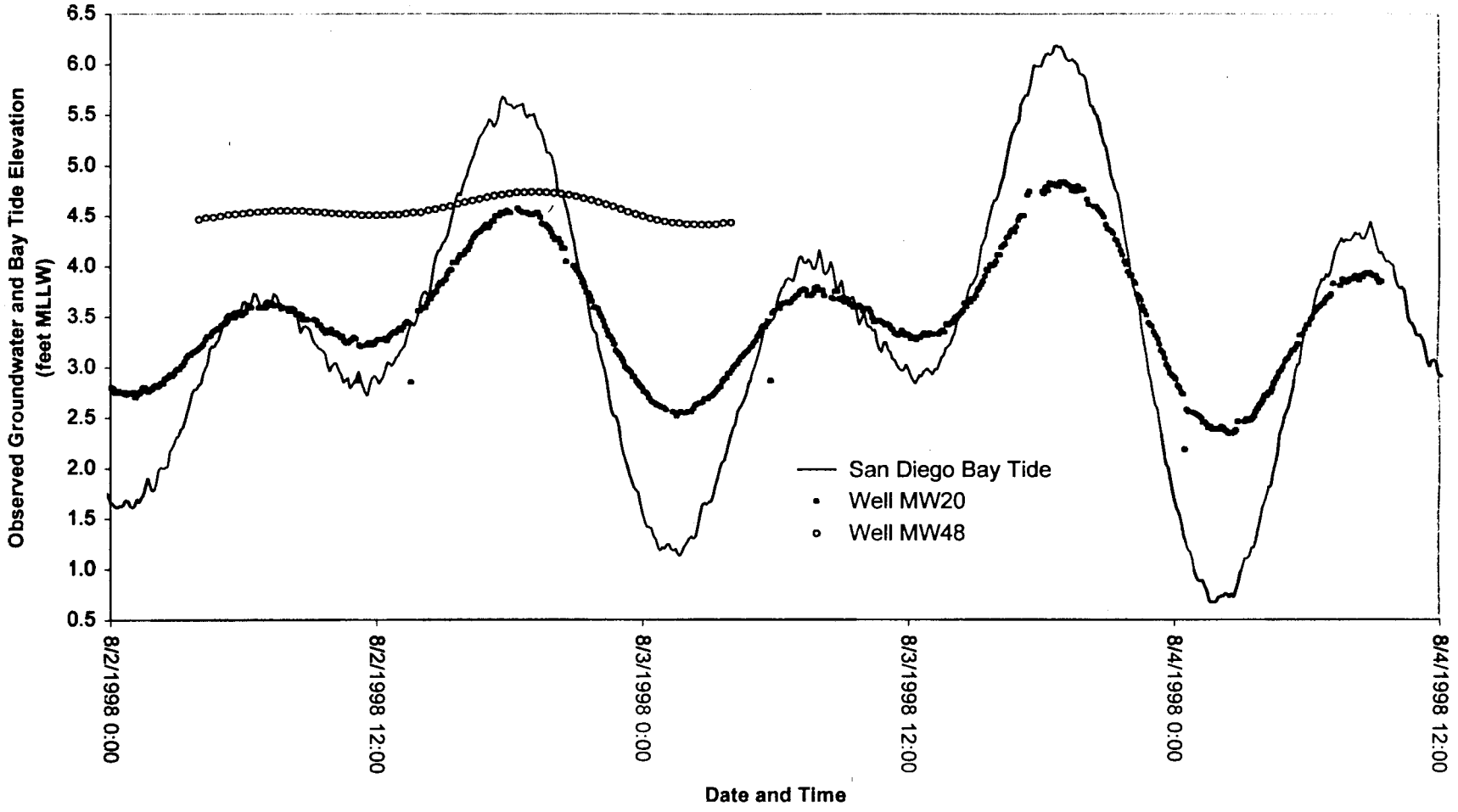

NAS NORTH ISLAND SITE 9
NoVOCs™ HYDROGEOLOGICAL INVESTIGATION

FIGURE 5-6
OBSERVED WATER LEVEL COMPARISON AMONG BAY TIDE, MW20 AND MW48

Tetra Tech EM Inc.

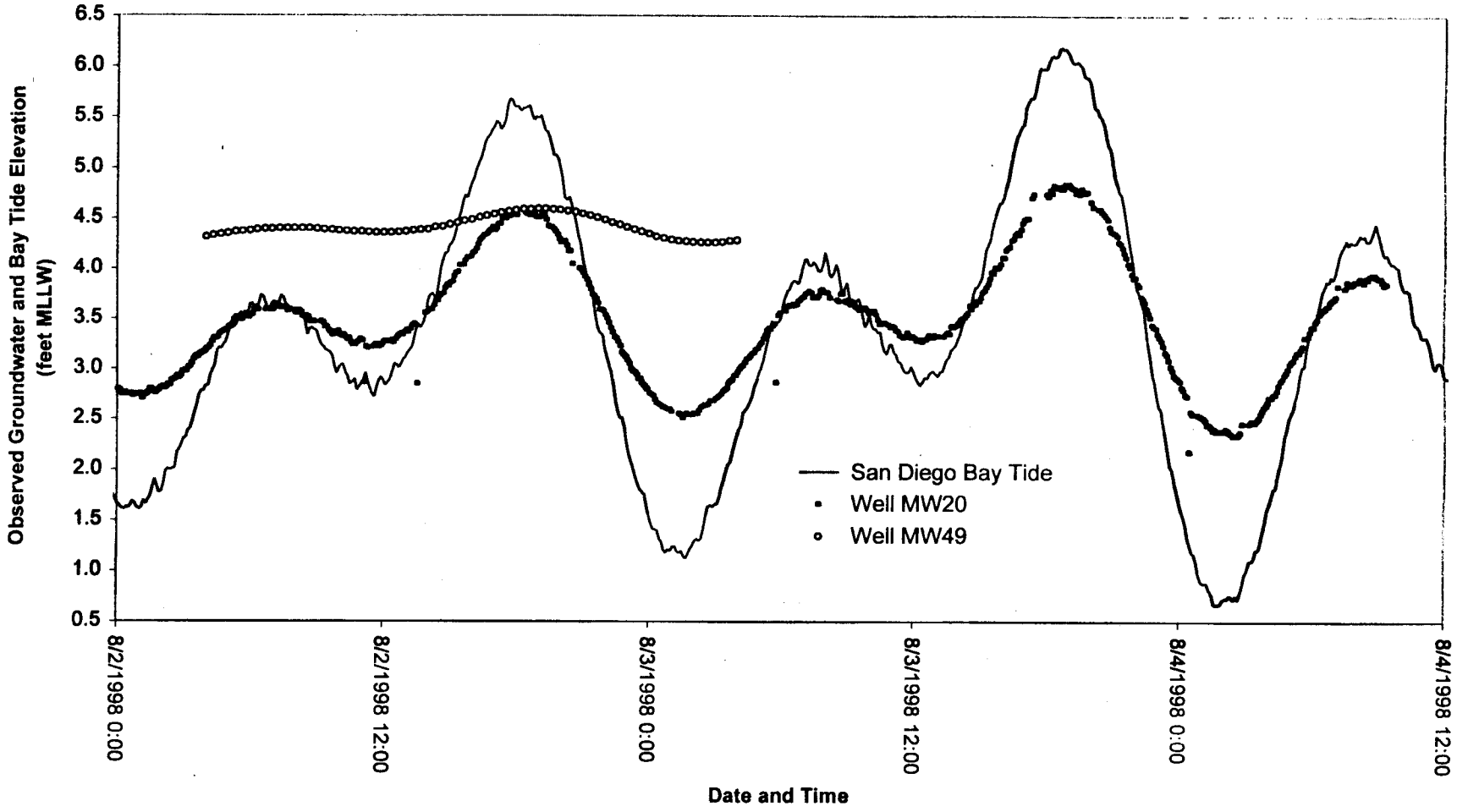

NAS NORTH ISLAND SITE 9
NoVOCs™ HYDROGEOLOGICAL INVESTIGATION

FIGURE 5-7
OBSERVED WATER LEVEL COMPARISON AMONG BAY TIDE, MW20 AND MW49

Tetra Tech EM Inc.

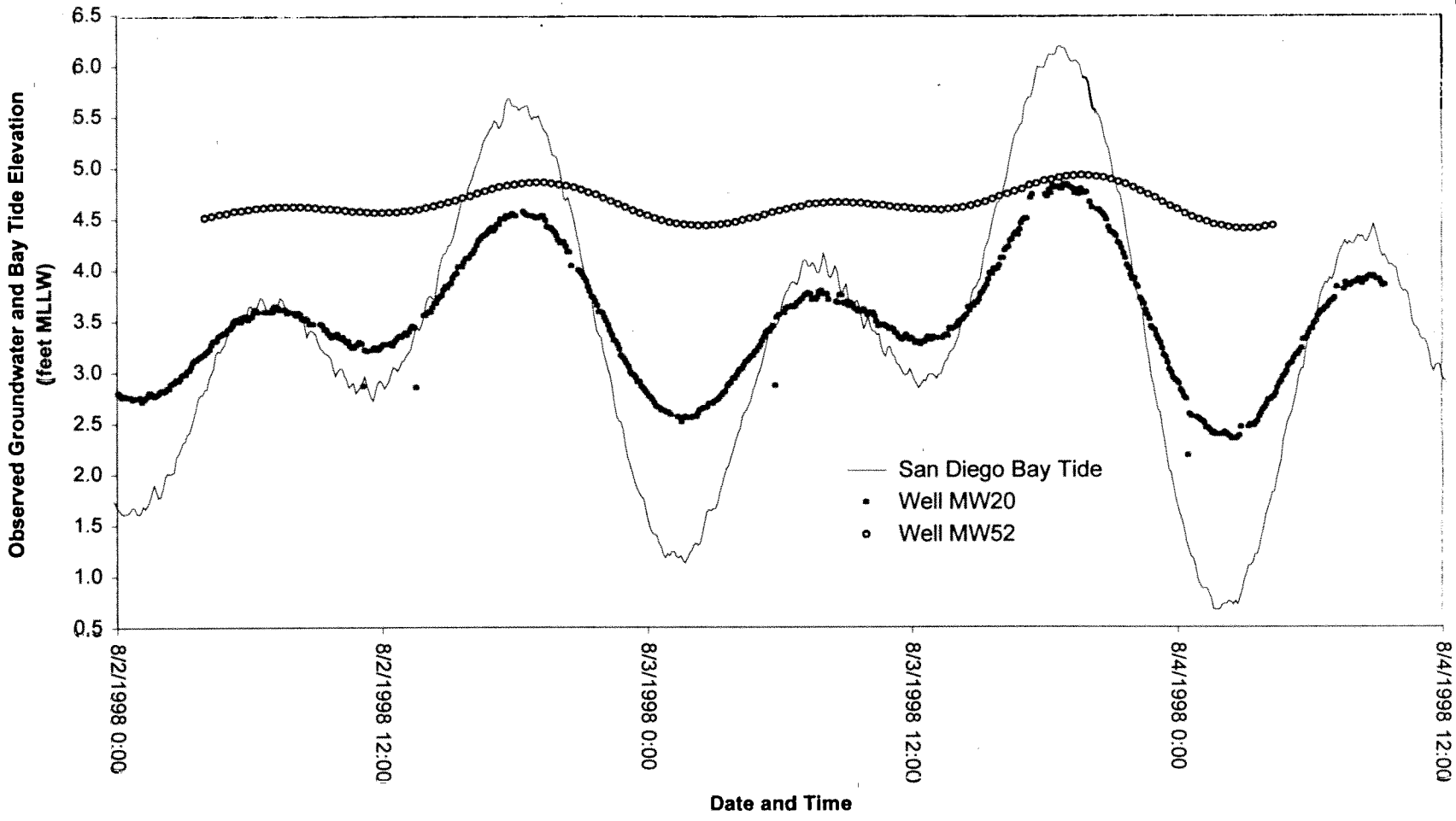

NAS NORTH ISLAND SITE 9
NoVOCs™ HYDROGEOLOGICAL INVESTIGATION

FIGURE 5-8
OBSERVED WATER LEVEL COMPARISON AMONG BAY TIDE, MW20 AND MW52

Tetra Tech EM Inc.

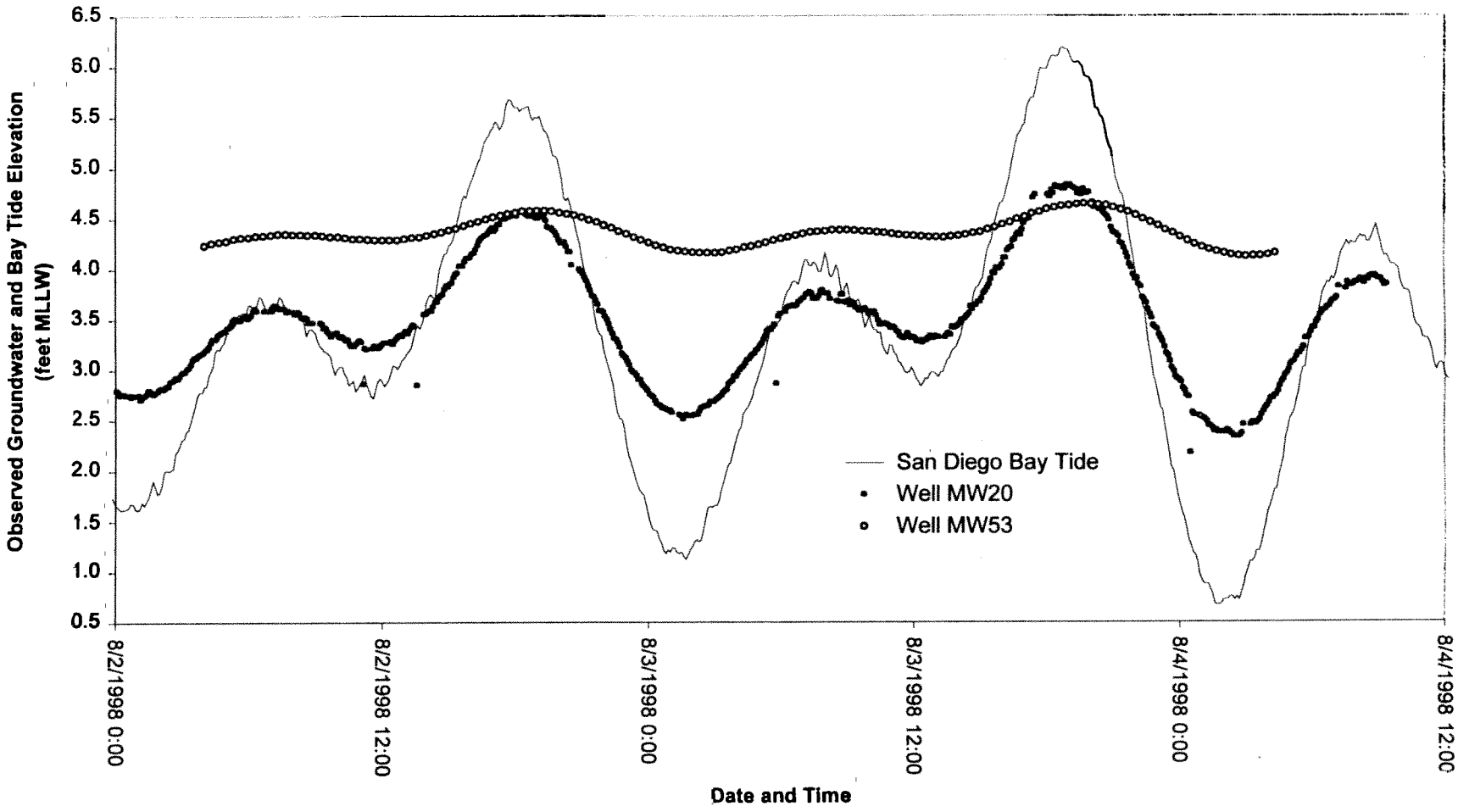

NAS NORTH ISLAND SITE 9
NoVOCs™ HYDROGEOLOGICAL INVESTIGATION

FIGURE 5-9
OBSERVED WATER LEVEL COMPARISON AMONG BAY TIDE, MW20 AND MW53

Tetra Tech EM Inc.